

Influence of Dopant-Host Energy Level Offset on Thermoelectric  
Properties of Doped Organic Semiconductors

Peer-reviewed author version

Nell, Bernhard; Ortstein, Katrin; Boltalina, Olga V. & VANDEWAL, Koen (2018)

Influence of Dopant-Host Energy Level Offset on Thermoelectric Properties of Doped  
Organic Semiconductors. In: JOURNAL OF PHYSICAL CHEMISTRY C, 122(22), p. 11730-11735.

DOI: 10.1021/acs.jpcc.8b03804

Handle: <http://hdl.handle.net/1942/27438>

# Influence of Dopant-Host Energy Level Offset on Thermoelectric Properties of Doped Organic Semiconductors

Bernhard Nell,<sup>\*,†</sup> Katrin Ortstein,<sup>†</sup> Olga V. Boltalina,<sup>‡</sup> and Koen Vandewal<sup>\*,†,¶</sup>

<sup>†</sup>*Dresden Integrated Center for Applied Physics and Photonic Materials, Technische  
Universität Dresden, 01062 Dresden, Germany*

<sup>‡</sup>*Department of Chemistry, Colorado State University, Fort Collins, CO 80523, USA*

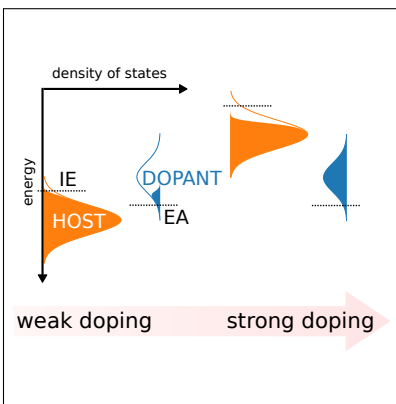
<sup>¶</sup>*Institute for Materials Research, IMEC-IMOMECA, Hasselt University, 3590 Diepenbeek,  
Belgium*

E-mail: bernhard.nell@iapp.de; koen.vandewal@uhasselt.be

## Abstract

Increasing the amount of charge carriers by molecular doping is important to improve the function of several organic electronic devices. In this work, we use highly fluorinated fullerene ( $C_{60}F_{48}$ ) to p-type dope common amorphous molecular host materials. We observe a general relation between the material's electrical conductivity and Seebeck coefficient, both strongly depending on the energy level offset between amorphous host and dopant. This suggests that the doping efficiency at similar doping levels is mainly determined by the electron transfer yield from host to dopant. Indeed, the dopant anion and host cation absorption strength correlate with the ionization energy (IE) of the host material. Host materials with an IE significantly below the electron affinity (EA) of the dopant yield the highest doping efficiency. Surprisingly, the doping efficiency reduces only by about one order of magnitude when the IE of the host material is increased by 0.55 eV, which we attribute to the disordered nature of the host materials

## Graphical TOC Entry



## Keywords

p-doping, organic, molecular doping, hole transport, Fullerene

Doping of small-molecule organic semiconductors had a major impact on the development of organic light emitting diodes (OLED) and organic photovoltaics (OPV).<sup>1-3</sup> Increasing the amount of mobile charge carriers in transparent layers at the contacts helps in reducing injection and extraction barriers and facilitates charge transport from absorber or to emission layers.<sup>4</sup> More recently it was shown that molecular doping can also significantly improve the electrical properties of polymers for thermoelectric and bio-electronic applications.<sup>5,6</sup> For optimized device performance it is therefore necessary to maximize the doping efficiency, namely the fraction of mobile charge carriers introduced per dopant and avoid charge carrier trapping or scattering at trap or dopant states possibly reducing the effective charge carrier mobility in the film. There are two factors detrimental for the performance of dopant-host systems. The first is a less-than-unity fraction of charges transferred between host and dopant.<sup>7-10</sup> The second is the fact that only a fraction of the created charge carriers is actually mobile and able to contribute to the electric current. The rest of the charges is immobilized in integer charge transfer complexes.<sup>11</sup> In contrast to inorganic doping, typical dopant concentrations in the percent range are required to introduce an amount of mobile charge carriers, sufficient for practical applications in OLEDs and solar cells.<sup>12,13</sup> However, the molecular factors determining efficient dopant-host systems are currently unknown. The performance of a dopant-host system is often evaluated by the increase in conductivity, which is not only affected by the increased charge carrier density with doping but also by the transport mechanism, energetic disorder and crystallinity of the investigated systems.<sup>14,15</sup> All these parameters heavily influence charge carrier mobility and a comparison based on electrical conductivity alone is often insufficient for a deeper mechanistic understanding. A combination of different techniques able to independently assess the density of carriers and the position of the Fermi-level or charge carrier mobility is therefore needed to study the influence of molecular parameters on the doping process itself. Only a few studies have systematically investigated the influence of the energy level offset between host and dopant on the doping efficiency so far. For efficient charge transfer, using dopants with

higher electron affinity compared to the ionization energy of the host was found to be beneficial in the case of p-type doping.<sup>7</sup> And while an influence of the electron affinity (EA) of tetracyanoquinodimethane (TCNQ) based molecules was observed,<sup>16</sup> a quantitative understanding of its influence is still missing. Similarly, in studies of n-doped C<sub>60</sub>, lower limits for the doping efficiency of various dopants were derived, but without investigating the role of the energy level alignment between host and dopant.<sup>17</sup> Here, we study a series of amorphous host materials with gradually increasing ionization energy (IE) to uncover its influence on the host-dopant charge transfer efficiency, conductivity and thermoelectric properties. The latter are closely related, since the Seebeck coefficient  $S$  at a temperature  $T$  depends on the Fermi-level position  $E_F$  and the energy dependent conductivity  $\sigma(E)$  through<sup>18</sup>

$$S = -\frac{1}{eT} \frac{\int_{-\infty}^{\infty} (E - E_F) \sigma(E) dE}{\int_{-\infty}^{\infty} \sigma(E) dE}. \quad (1)$$

The Seebeck coefficient contains therefore only information on the carriers contributing to conductivity. In order to characterize the total amount of (mobile and trapped) charges introduced by the dopant, we use UV-VIS-NIR absorption measurements to characterize the relative density of transferred carriers from their optical signatures and relate them to the thermoelectric properties. By combining these methods it is possible to investigate the influence of molecular parameters, i.e., the IE of the host materials determined by UPS, on the doping efficiency. We study relevant materials, which are used in vacuum deposited OLEDs and OPV, in particular, typical small-molecule hole transport materials N,N'-Di(naphthalen-1-yl)-N,N'-diphenyl-benzidine ( $\alpha$ -NPD), N,N'-((Diphenyl-N,N'-bis)9,9-dimethyl-fluoren-2-yl)-benzidine (BF-DPB), 9,9-bis[4-(N,N-bis-biphenyl-4-yl-amino)phenyl]-9H-fluorene (BPAPF) and 4,4',4''-tris(carbazol-9-yl)-triphenylamine (TCTA),<sup>19,20</sup> all based on triphenylamine building blocks. The IE of these hosts change approximately in steps of 0.1-0.2 eV and are higher (lower) than the EA of the dopants used in this study. We find that increasing energy level offset between host and dopant leads to a strongly reduced doping

efficiency. Nevertheless, even when increasing the ionization energy by as much as 0.55 eV significant charge transfer and an increase in conductivity can still be observed. However, to achieve the highest doping efficiency, the electron affinity must be sufficiently high, above the ionization energy of the host.

TCTA and  $\alpha$ -NPD are well studied materials, mainly used in OLED applications, while BF-DPB and BPAPF are more commonly found in transport layers of organic solar cells. All host materials predominantly form amorphous layers. The ionization energy measured by ultra-violet photoelectron spectroscopy in thin films gradually changes from 5.85 eV for TCTA, 5.6 eV for BPAPF, 5.45 eV for  $\alpha$ -NPD to 5.3 eV for BF-DPB (Figure 1). The host

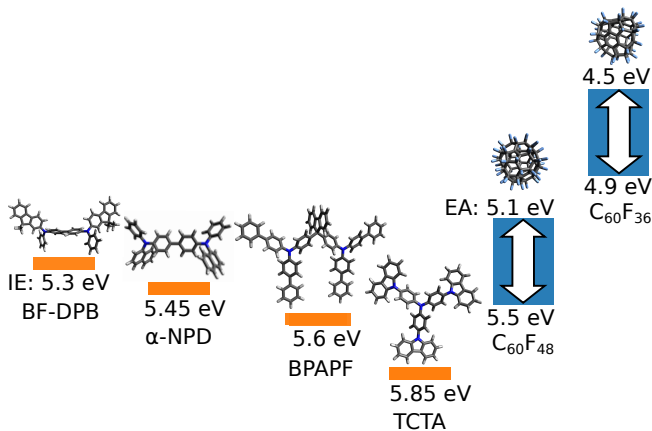


Figure 1: The ionization energies of the hosts measured by UPS gradually change from 5.3 to 5.85 eV. Electron affinities ranging from 5.1 to 5.5 eV are reported for  $C_{60}F_{48}$ , while 0.6 eV lower values are observed for  $C_{60}F_{36}$ .

materials are doped with the fluorinated fullerene dopant  $C_{60}F_{48}$  at different doping concentrations. Depending on the characterization method a range of values for the EA of  $C_{60}F_{48}$  is reported literature. The EA of fluorinated fullerenes shift due to fluorination, showing a linear dependence on the number of fluorine atoms. The gas-phase EA value determined for  $C_{60}F_{48}$  by Fourier transform ion cyclotron mass spectrometry (FTMS) bracketing method is reported as 4.1(3) eV,<sup>21</sup> which is 1.3 eV higher than the EA of  $C_{60}F_2$ ,<sup>22</sup> while a shift from 2.7 eV of  $C_{60}$  to 5.0 eV and 5.6 eV in the case of open-shell species  $C_{60}F_{35}$  and  $C_{60}F_{47}$  re-

spectively was determined by photoelectron spectroscopy.<sup>23</sup> A similar trend was observed in CV measurements, where a LUMO shift 0.58 eV was derived from the half-wave reduction potentials, when increasing the number of fluorine atoms from 36 to 48,<sup>24</sup> whereas the CV-derived LUMO shift from C<sub>60</sub> to C<sub>60</sub>F<sub>48</sub> was reported as 1.38 eV.<sup>25</sup> While these values are not always comparable to thin-film electron affinities, the EA of C<sub>60</sub>F<sub>48</sub> determined from surface doping experiments was found to be higher than that of the more commonly used dopant F4-TCNQ with an EA between 5.1 to 5.4 eV.<sup>26–29</sup> An estimation of the electron affinity from electrochemical potentials and the electron affinity of C<sub>60</sub> from inverse photoelectron spectroscopy (IPES) measurements on thin films<sup>30–34</sup> yields a similar value of roughly 5.5 eV. This suggests that the LUMO energy of C<sub>60</sub>F<sub>48</sub> is close to the energy of the highest occupied molecular orbital (HOMO) of BF-DPB, the host material with the lowest IE used in this study, which is also doped with C<sub>60</sub>F<sub>36</sub>. HOMO (LUMO) refers here to the energetic position of the maximum in a disordered density of states, while IE (EA) is usually determined from the onset as specified in the supporting information.

For all C<sub>60</sub>F<sub>48</sub>-doped host materials, with molar dopant-host ratios from 0.001 to 0.1, we find an increasing electrical conductivity with increasing doping concentration (Figure 2). At the same time, the Seebeck coefficient decreases significantly from approximately

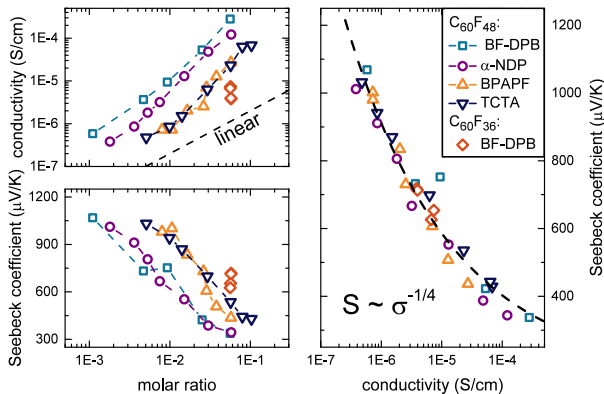


Figure 2: Electrical conductivity and Seebeck coefficient of the investigated dopant-host systems. Seebeck coefficient and conductivity are strongly related, independent of the material combination. As the ionization energy of the host increases, the conductivity is reduced and the Seebeck coefficient increases.

1000  $\mu\text{V}/\text{K}$  at the lowest doping concentration to 300  $\mu\text{V}/\text{K}$  at high concentrations. All samples show a positive Seebeck coefficient indicating hole transport and p-type doping. Comparing the different systems at similar dopant-host stoichiometries, we find significant differences, with higher IE host materials exhibiting a reduced conductivity and increased Seebeck coefficient. Nevertheless, even the highest IE material, TCTA, shows a significantly increased conductivity upon doping with  $\text{C}_{60}\text{F}_{48}$ . At the same molar ratio, the conductivity of BF-DPB is roughly one order of magnitude higher than that of TCTA. The superlinear conductivity increase with doping concentration observed in all systems is an indication for the presence of tail states that are subsequently filled upon doping.<sup>12</sup> Despite the wide range of conductivities spanning three orders of magnitude, its relation with the Seebeck coefficient is very similar for all materials, following an apparent power law dependence of  $S \sim \sigma^{-1/4}$ , as it has been observed before in the case of doped polymers.<sup>35</sup> This behavior is characteristic for materials that are dominated by static disorder.<sup>36</sup> The fact that we observe this relation with only little variation for all materials indicates that energetic disorder and reorganization energies are very similar in the investigated host materials. The differences in Seebeck coefficient and conductivity for different hosts are therefore solely related to the total density of mobile charge carriers introduced by the dopant. This is also valid when  $\text{C}_{60}\text{F}_{48}$  is exchanged by the weaker dopant  $\text{C}_{60}\text{F}_{36}$ .<sup>37,38</sup> When  $\text{C}_{60}\text{F}_{36}$  is doped in BF-DPB, we observe a significantly higher Seebeck coefficient and lower conductivity.

As we have established above that the differences in conductivity and Seebeck coefficient must come from a different number of mobile carriers introduced by the dopant, we now use optical spectroscopy to determine trends in the fraction of charges transferred. While undoped, only a single absorption feature for wavelengths around 400 nm is visible for all host systems. Upon doping with  $\text{C}_{60}\text{F}_{48}$ , new features, slightly red-shifted as compared to the main absorption peak, appear, together with a broad near-infrared absorption (Figure S1). Such features have been previously attributed to cation absorption in triphenylamine-based molecules<sup>39-42</sup> and indicate integer charge transfer from host to dopant. Cation absorption

is also found when the IE is as high as 5.85 eV in the case of TCTA. No characteristic absorption peaks of  $C_{60}F_{48}$  molecules are visible in the investigated wavelength range from 290 to 2500 nm due to its large optical gap.<sup>43</sup> A similar behavior was observed in MeO-TPD doped with  $C_{60}F_{36}$ .<sup>44</sup> The doping related absorption increases with doping concentration and is the strongest for the lowest IE materials BF-DPB and  $\alpha$ -NPD, while changes are hardly visible in BF-DPB doped with  $C_{60}F_{36}$  (Figure S2), even at the highest doping concentration at a molar ratio (MR) of 0.2. In recent studies, no significant amount of charge transfer was observed when doping TCTA with F6-TCNNQ, even though a thin-film electron affinity of 5.6 eV was determined.<sup>16,45</sup> This suggests an improved doping strength of  $C_{60}F_{48}$ , as compared to more commonly used dopants F4-TCNQ, F6-TCNNQ and  $C_{60}F_{36}$ . The clearly visible cation features in the absorption spectra of  $C_{60}F_{48}$ -doped samples allow an estimation of the relative fraction of dopant induced charges by comparing their integrated absorbance. Since neither  $C_{60}F_{48}$  nor its anion show any characteristic absorption features in the investigated wavelength range, the molar absorptivity of the NIR peaks is estimated using CN6-CP with a LUMO energy of 5.87 eV as a dopant.<sup>46</sup> This molecule has a characteristic anion absorption that can be used as a reference (detailed evaluation in Supporting Information) by comparing the integrated dopant anion and NIR cation absorption of the host materials.

The estimated charge transfer efficiency relative to the lowest IE host BF-DPB, which exhibits the highest degree of charge transfer to the dopant is shown in Figure 3. Increasing the ionization energy from 5.3 eV to 5.85 eV leads to a reduction of the charge transfer efficiency by a factor of 10 in the  $C_{60}F_{48}$ -doped films, while a slightly reduced charge transfer efficiency can already be observed when the IE is increased by 0.15 eV. It may seem surprising, that even when the HOMO of the host is significantly lower than the LUMO of the dopant, as much as 0.55 eV, integer charge transfer and a conductivity increase can still be observed. This rather slow decay in charge transfer efficiency can be rationalized by the strong disorder of the investigated host materials in the order of hundred meV,<sup>9</sup> as found in UPS measurements (Table S7). Furthermore, the relative charge transfer efficiency

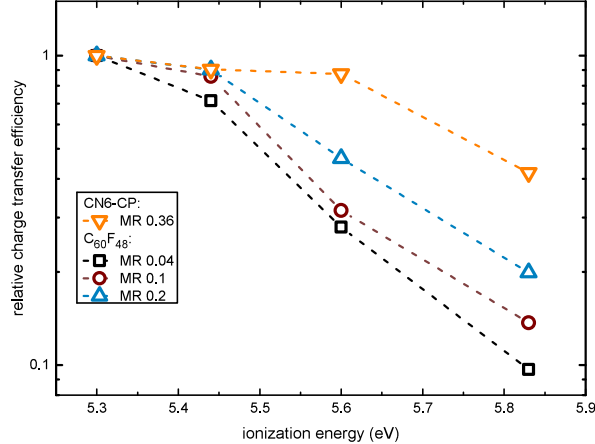


Figure 3: Relative charge transfer efficiency as a function of ionization energy. Increasing the ionization energy reduces the charge transfer efficiency estimated from UV-VIS-NIR measurements of  $C_{60}F_{48}$ -doped films. Using CN6-CP, a reduced charge transfer efficiency is only observed at IE above 5.6 eV

increases with doping concentration. While this behavior seems counter-intuitive at first, it is explained by a further broadening of the density of states occurring at high doping concentrations.<sup>47,48</sup> This trend is reproduced when calculating charge transfer by solving charge neutrality equation for Gaussian density of states numerically<sup>49</sup> (Figure S9). Comparing the anion absorption peaks of CN6-CP-doped samples, we find that the charge transfer efficiency is comparably high in BF-DPB,  $\alpha$ -NPD and BPAPF but reduced by a factor of 2 in TCTA. Both dopants,  $C_{60}F_{48}$  and CN-6CP, show significant charge transfer even in TCTA, which, in the case of molecular doping, has only been reported for transition metal oxides so far.<sup>50</sup> The drop in charge transfer efficiency occurs at 0.3 to 0.4 eV higher ionization energies compared to  $C_{60}F_{48}$ , hinting at a difference in their EA of the same magnitude. As the difference between the LUMO levels of CN6-CP and F6-TCNNQ is reported to be in the range of 0.5 to 0.6 eV<sup>46,51</sup> an estimation from our optical measurements yields an EA of  $C_{60}F_{48}$  in the range of 5.8 eV, slightly higher than F6-TCNNQ. Within the limitations to accurately determine the electron affinity this agrees very well with the lower doping strength observed of F6-TCNNQ in TCTA.<sup>45</sup> Correcting the doping concentration by the relative intensities we can relate charge carriers introduced by doping to the fraction of mobile charge

carriers by plotting the conductivity and Seebeck coefficient as a function of the relative carrier density. We find that the electrical properties are comparable at similar charge carrier densities, independent of the host material. This supports the idea that the differences in Seebeck coefficient and electrical conductivity measured at different doping concentrations, and therefore in doping efficiency, are indeed caused by the different degree of charge transfer that originates from the IE differences. The doping efficiency of TCTA is slightly lower than expected from the thermopower-conductivity relation, however, the spread of conductivity and Seebeck coefficient between different materials is significantly reduced (Figure 4).

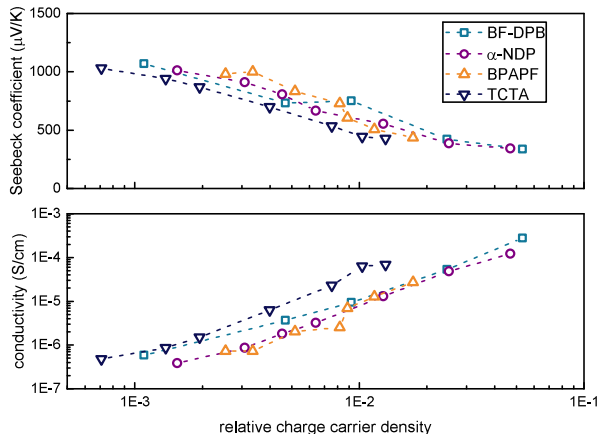


Figure 4: Conductivity and Seebeck coefficient as a function of relative charge carrier density. The relative charge carrier density was calculated from the molar doping ratio and the relative charge transfer efficiency determined from absorption measurements at a molar ratio of 0.1.

Even though structural relaxation might change the energy level offset leading to a different doping efficiency than anticipated from the energy levels of the isolated materials<sup>52–54</sup>, the observed trend of the CT efficiency with the change in IE is clear. For a more detailed insight a determination of the host-dopant electronic structure in a blend film is preferable but experimentally challenging.

In summary, using the highly fluorinated dopant  $C_{60}F_{48}$  it is possible to dope and investigate the thermoelectrical and optical properties of amorphous hole transport materials with ionization energies as high as 5.85 eV. Comparing optical and electrical measurements we find that the electrical conductivity and Seebeck coefficient are strongly related in the inves-

tigated systems. Differences found at the same molar ratio originate from a different fraction of ionized dopants, leading us to the conclusion that the amount of charges transferred mainly depends on the energy level difference between host and dopant and that other properties such as the width of the densities of states and transport mechanisms are very similar in the investigated hole transport materials, typically used in vacuum deposited OLEDs or OPV. The steady decay in doping efficiency observed when increasing the ionization energy highlights the importance of the energy level alignment in the case of integer charge transfer to achieve the highest doping efficiency. However, due to the energetic disorder present in the investigated materials, polaron absorption originating from charge transfer can be observed in a broad energy range, even at large energy level offsets. The still high charge transfer efficiency of both dopants, CN6-CP and  $C_{60}F_{48}$ , in TCTA makes them promising candidates for the electrical doping of other host materials with similarly high IE.

## Experimental

The dopant material,  $C_{60}F_{48}$ , was synthesized by direct fluorination of 99.8%  $C_{60}$  (MTR Co.) with  $F_2$  gas at elevated temperatures as described elsewhere.<sup>55,56</sup> The sample was analyzed by negative-ion atmospheric pressure chemical ionization mass spectrometry (2000 Finnigan LCQ-DUO mass-spectrometer),  $^{19}F$  NMR (Varian INOVA 400 MHz) and HPLC (Shimadzu LC-6AD with a SPD-201A UV-VIS detector, Japan) which showed 98%+ compositional purity and 95%+ isomeric purity of  $D_3$ - $C_{60}F_{48}$  (with a minor  $C_{60}F_{48}$  isomer of  $S_6$  symmetry). No further purification was done.  $C_{60}F_{36}$  dopant was prepared using previously described method<sup>57</sup> and characterized to be 98%+ compositional purity (consisting of one major isomer of  $C_3$ -symmetry and two minor ones of  $C_1$  and T-symmetry), after purification by sublimation. TCTA and  $\alpha$ -NPD were purchased from Sensient, BF-DPB and BPAPF from Synthon and Lumtec, respectively. All hole transport materials were sublimed at least twice before being processed. The doped films were prepared on glass substrates under vac-

uum atmosphere at pressures of approximately  $10^{-7}$  mbar by thermal co-evaporation of host and dopant. The deposition was monitored using separate quartz microbalances. Typically films with a total thickness of 60 nm were prepared at deposition rates of  $0.3 \text{ \AA}/\text{s}$  for electrical characterization, while in the optical characterization films with a constant thickness of the host of 100 nm was used. Electrodes of 20 mm width were deposited prior to the organic materials at a distance of 5 mm using 40 nm of gold on top of a 3 nm chromium seed layer. After the deposition the films were heated for four hours at  $90 \text{ }^\circ\text{C}$  ( $80 \text{ }^\circ\text{C}$  in the case of  $\alpha$ -NPD due to the low glass transition temperature) to ensure that a stable film configuration was reached. Thermovoltage and electrical conductivity were measured in-situ using a Keithley 236 SMU without breaking vacuum. The Seebeck coefficient was determined at a temperature gradient of 5 K, electrical conductivity was measured at a voltage of 1 V. Absorption measurements were performed in air using a Shimadzu SolidSpec-3700 UV-VIS-NIR. The absorption of a reference glass substrate was subtracted from all measurements. The IE of the intrinsic host materials was determined by UPS. Spectra were recorded with a PHOIBOS 100 analyzer system (Specs, Berlin, Germany) at base pressures of  $10^{10}$  mbar. He I excitation lines (21.22 eV) from helium discharge lamp were used as illumination source. The energy resolution of the System was determined as 150 meV. Samples were prepared on silver substrates at thicknesses of 20 nm. The IE is obtained from the sum of the work function and the HOMO onset.

## Acknowledgement

KV and BN thank the "Thinface" project from the European Union Seventh Framework Programme (no. 607232) and the Graduate Academy of TU Dresden for financial support. OVB thanks National Science Foundation for partial support (grant CHE-1362302). The authors thank L.Shi and Y.Liu for recording absorption spectra of TCTA and doped BF-DPB and Y.Karpov and A. Kiriya for providing CN6-CP dopant.

## Supporting Information Available

The following files are available free of charge.

- supporting\_information.pdf: Recorded UV-VIS-NIR spectra, detailed evaluation of absorbance spectra, numerical calculation of charge transfer efficiency, UPS spectra

## References

- (1) Blochwitz, J.; Pfeiffer, M.; Fritz, T.; Leo, K. Low voltage organic light emitting diodes featuring doped phthalocyanine as hole transport material. *Appl. Phys. Lett.* **1998**, *73*.
- (2) Männig, B.; Gebeyehu, D.; Simon, P.; Kozlowski, F.; Werner, A.; Li, F.; Grundmann, S.; Sonntag, S.; Koch, M.; Leo, K. et al. Organic p-i-n solar cells. *Appl. Phys. A* **2004**, *79*, 1–14.
- (3) Walzer, K.; Männig, B.; Pfeiffer, M.; Leo, K. Highly efficient organic devices based on electrically doped transport layers. *Chem. Rev.* **2007**, *107*, 1233–1271.
- (4) Blochwitz, J.; Fritz, T.; Pfeiffer, M.; Leo, K.; Alloway, D. M.; Lee, P. A.; Armstrong, N. R. Interface electronic structure of organic semiconductors with controlled doping levels. *Org. Electron.* **2001**, *2*, 97–104.
- (5) Kim, G. H.; Shao, L.; Zhang, K.; Pipe, K. P. Engineered doping of organic semiconductors for enhanced thermoelectric efficiency. *Nat. Mater.* **2013**, *12*, 719–723.
- (6) Liao, C.; Zhang, M.; Yao, M. Y.; Hua, T.; Li, L.; Yan, F. Flexible Organic Electronics in Biology: Materials and Devices. *Adv. Mater.* **2015**, *27*, 7493–7527.
- (7) Pfeiffer, M.; Leo, K.; Zhou, X.; Huang, J. S.; Hofmann, M.; Werner, A.; Blochwitz-Nimoth, J. Doped organic semiconductors: Physics and application in light emitting diodes. *Org. Electron.* **2003**, *4*, 89.

- (8) Salzmann, I.; Heimel, G.; Duhm, S.; Oehzelt, M.; Pingel, P.; George, B. M.; Schnegg, A.; Lips, K.; Blum, R. P.; Vollmer, A. et al. Intermolecular hybridization governs molecular electrical doping. *Phys. Rev. Lett.* **2012**, *108*, 035502.
- (9) Salzmann, I.; Heimel, G.; Oehzelt, M.; Winkler, S.; Koch, N. Molecular Electrical Doping of Organic Semiconductors: Fundamental Mechanisms and Emerging Dopant Design Rules. *Acc. Chem. Res.* **2016**, *49*, 370–378.
- (10) Tietze, M. L.; Pahner, P.; Schmidt, K.; Leo, K.; Lüssem, B. Doped organic semiconductors: Trap-filling, impurity saturation, and reserve regimes. *Adv. Func. Mater.* **2015**, *25*, 2701–2707.
- (11) Tietze, M. L.; Benduhn, J.; Pahner, P.; Nell, B.; Schwarze, M.; Kleemann, H.; Kramer, M.; Zojer, K.; Vandewal, K.; Leo, K. Elementary steps in electrical doping of organic semiconductors. *Nat. Comm.* **2018**, *9*.
- (12) Olthof, S.; Mehraeen, S.; Mohapatra, S. K.; Barlow, S.; Coropceanu, V.; Brédas, J. L.; Marder, S. R.; Kahn, A. Ultralow doping in organic semiconductors: Evidence of trap filling. *Phys. Rev. Lett.* **2012**, *109*.
- (13) Mityashin, A.; Olivier, Y.; Van Regemorter, T.; Rolin, C.; Verlaak, S.; Martinelli, N. G.; Beljonne, D.; Cornil, J.; Genoe, J.; Heremans, P. Unraveling the mechanism of molecular doping in organic semiconductors. *Adv. Mater.* **2012**, *24*, 1535–1539.
- (14) Baranovskii, S. D. Theoretical description of charge transport in disordered organic semiconductors. *Phys. Status Solidi B* **2014**, *251*, 487–525.
- (15) Rivnay, J.; Jimison, L. H.; Northrup, J. E.; Toney, M. F.; Noriega, R.; Lu, S.; Marks, T. J.; Facchetti, A.; Salleo, A. Large modulation of carrier transport by grain-boundary molecular packing and microstructure in organic thin films. *Nat. Mater.* **2009**, *8*, 952–958.

- (16) Méndez, H.; Heimel, G.; Winkler, S.; Frisch, J.; Opitz, A.; Sauer, K.; Wegner, B.; Oehzelt, M.; Röthel, C.; Duhm, S. et al. Charge-transfer crystallites as molecular electrical dopants. *Nat. Commun.* **2015**, *6*.
- (17) Menke, T.; Ray, D.; Kleemann, H.; Leo, K.; Riede, M. Determining doping efficiency and mobility from conductivity and Seebeck data of n-doped C<sub>60</sub> layers. *Phys. Status Solidi B* **2015**, *252*, 1877–1883.
- (18) Fritzsche, H. A general expression for the thermoelectric power. *Solid State Commun.* **1971**, *9*, 1813–1815.
- (19) Kuwabara, Y.; Ogawa, H.; Inada, H.; Noma, N.; Shirota, Y. Thermally stable multired organic electroluminescent devices using novel starburst molecules, 4,4',4''-Tri(N-carbazolyl)triphenylamine (TCTA) and 4,4',4''-Tris(3-methylphenylphenylamino)triphenylamine (m-MTDATA), as hole-transport materials. *Adv. Mater.* **1994**, *6*, 677–679.
- (20) Ko, C. W.; Tao, Y. T. 9,9-bis{4-[di-(p-biphenyl)aminophenyl]}fluorene: A high T<sub>g</sub> and efficient hole-transporting material for electroluminescent devices. *Synth. Met.* **2002**, *126*, 37–41.
- (21) Jin, C.; Hettich, R. L.; Compton, R. N.; Tuinman, A.; Derecskei-Kovacs, A.; Marynick, D. S.; Dunlap, B. I. Attachment of two electrons to C<sub>60</sub>F<sub>48</sub>: Coulomb barriers in doubly charged anions. *Phys. Rev. Lett.* **1994**, *73*, 2821–2824.
- (22) Boltalina, O. V.; Ponomarev, D. B.; Sidorov, L. N. Thermochemistry of fullerene anions in the gas phase. *Mass Spectrom. Rev.* **1997**, *16*, 333–351.
- (23) Wang, X. B.; Chi, C.; Zhou, M.; Kuvychko, I. V.; Seppelt, K.; Popov, A. A.; Strauss, S. H.; Boltalina, O. V.; Wang, L. S. Photoelectron spectroscopy of C<sub>60</sub>F<sub>n</sub><sup>-</sup> and C<sub>60</sub>F<sub>m</sub><sup>2-</sup> (n = 17, 33, 35, 43, 45, 47; m = 34, 46) in the gas phase and the generation

- and characterization of  $C_1-C_{60}F_{47}^-$  and  $D_2-C_{60}F_{44}$  in solution. *J. Phys. Chem. A* **2010**, *114*, 1756–1765.
- (24) Liu, N.; Morio, Y.; Okino, F.; Touhara, H.; Boltalina, O. V.; Pavlovich, V. K. Electrochemical properties of  $C_{60}F_{36}$ . *Synth. Met.* **1997**, *86*, 2289–2290.
- (25) Zhou, F.; Van Berkel, G. J.; Donovan, B. T. Electron-Transfer Reactions of  $C_{60}F_{48}$ . *J. Am. Chem. Soc.* **1994**, *116*, 5485–5486.
- (26) Paterson, A. F.; Lin, Y.-H.; Mottram, A. D.; Fei, Z.; Niazi, M. R.; Kirmani, A. R.; Amassian, A.; Solomeshch, O.; Tessler, N.; Heeney, M. et al. The Impact of Molecular p-Doping on Charge Transport in High-Mobility Small-Molecule/Polymer Blend Organic Transistors. *Adv. Electron. Mater.* **2017**, 1700464.
- (27) Edmonds, M. T.; Wanke, M.; Tadich, A.; Vulling, H. M.; Rietwyk, K. J.; Sharp, P. L.; Stark, C. B.; Smets, Y.; Schenk, A.; Wu, Q. H. et al. Surface transfer doping of hydrogen-terminated diamond by  $C_{60}F_{48}$ : Energy level scheme and doping efficiency. *J. Chem. Phys.* **2012**, *136*, 124701.
- (28) Smets, Y.; Stark, C. B.; Schmitt, F.; Edmonds, M. T.; Lach, S.; Wright, C. A.; Langley, D. P.; Rietwyk, K. J.; Schenk, A.; Tadich, A. et al. Doping efficiency and energy-level scheme in  $C_{60}F_{48}$ -doped zinc-tetraphenylporphyrin films. *Org. Electron.* **2013**, *14*, 169–174.
- (29) Tadich, A.; Edmonds, M. T.; Ley, L.; Fromm, F.; Smets, Y.; Mazej, Z.; Riley, J.; Pakes, C. I.; Seyller, T.; Wanke, M. Tuning the charge carriers in epitaxial graphene on SiC(0001) from electron to hole via molecular doping with  $C_{60}F_{48}$ . *Appl. Phys. Lett.* **2013**, *102*, 241601.
- (30) Akaike, K.; Kanai, K.; Yoshida, H.; Tsutsumi, J.; Nishi, T.; Sato, N.; Ouchi, Y.; Seki, K. Ultraviolet photoelectron spectroscopy and inverse photoemission spectroscopy of [6,6]-

- phenyl-C<sub>61</sub>-butyric acid methyl ester in gas and solid phases. *J. Appl. Phys.* **2008**, *104*, 023710.
- (31) Zhao, W.; Kahn, A. Charge transfer at n-doped organic-organic heterojunctions. *J. Appl. Phys.* **2009**, *105*, 123711.
- (32) Guan, Z. L.; Kim, J. B.; Wang, H.; Jaye, C.; Fischer, D. A.; Loo, Y. L.; Kahn, A. Direct determination of the electronic structure of the poly(3-hexylthiophene):phenyl-[6,6]-C<sub>61</sub> butyric acid methyl ester blend. *Org. Electron.* **2010**, *11*, 1779–1785.
- (33) Kanai, K.; Akaike, K.; Koyasu, K.; Sakai, K.; Nishi, T.; Kamizuru, Y.; Nishi, T.; Ouchi, Y.; Seki, K. Determination of electron affinity of electron accepting molecules. *Appl. Phys. A* **2009**, *95*, 309–313.
- (34) Schwedhelm, R.; Kipp, L.; Dallmeyer, A.; Skibowski, M. Experimental band gap and core-hole electron interaction in epitaxial C<sub>60</sub> films. *Phys. Rev. B* **1998**, *58*, 13176–13180.
- (35) Glauddell, A. M.; Cochran, J. E.; Patel, S. N.; Chabinyk, M. L. Impact of the doping method on conductivity and thermopower in semiconducting polythiophenes. *Adv. Energy Mater.* **2015**, *5*, 1401072.
- (36) Abdalla, H.; Zuo, G.; Kemerink, M. Range and energetics of charge hopping in organic semiconductors. *Phys. Rev. B* **2017**, *96*.
- (37) Meerheim, R.; Olthof, S.; Hermenau, M.; Scholz, S.; Petrich, A.; Tessler, N.; Solomeshch, O.; Lüssem, B.; Riede, M.; Leo, K. Investigation of C<sub>60</sub>F<sub>36</sub> as low-volatility p-dopant in organic optoelectronic devices. *J. Appl. Phys.* **2011**, *109*, 103102.
- (38) Menke, T.; Ray, D.; Kleemann, H.; Hein, M. P.; Leo, K.; Riede, M. Highly efficient p-dopants in amorphous hosts. *Org. Electron.* **2014**, *15*, 365–371.

- (39) Coropceanu, V.; Lambert, C.; Nöll, G.; Brédas, J. L. Charge-transfer transitions in triarylamine mixed-valence systems: The effect of temperature. *Chem. Phys. Lett.* **2003**, *373*, 153–160.
- (40) Baasanjav, S.; Bolormaa, G.; Naranbileg, B.; Battulga, M.; Ganzorig, C. Spectroelectrochemical Study of the Formation of Radical cations of 4,4'-bis[N-(1-naphthyl)-N-phenyl-amino]-biphenyl as a Hole Transport Semiconductor Material. *MRS Proc.* **2011**, *1286*, mrsf10-1286-e03-16.
- (41) Karon, K.; Lapkowski, M.; Dabulienė, A.; Tomkeviciene, A.; Kostiv, N.; Grazulevičius, J. V. Spectroelectrochemical characterization of conducting polymers from star-shaped carbazole-triphenylamine compounds. *Electrochim. Acta* **2015**, *154*, 119–127.
- (42) Kröger, M.; Hamwi, S.; Meyer, J.; Riedl, T.; Kowalsky, W.; Kahn, A. Role of the deep-lying electronic states of MoO<sub>3</sub> in the enhancement of hole-injection in organic thin films. *Appl. Phys. Lett.* **2009**, *95*, 253504–123301.
- (43) Boltalina, O. V.; Sidorov, L. N.; Bagryantsev, V. F.; Seredenko, V. A.; Zapol'skii, A. S.; Street, J. M.; Taylor, R. Formation of C<sub>60</sub>F<sub>48</sub> and fluorides of higher fullerenes. *J. Chem. Soc., Perkin Trans 2* **1996**, 2275.
- (44) Li, J.; Rochester, C. W.; Jacobs, I. E.; Friedrich, S.; Stroeve, P.; Riede, M.; Moulé, A. J. Measurement of Small Molecular Dopant F4TCNQ and C<sub>60</sub>F<sub>36</sub> Diffusion in Organic Bilayer Architectures. *ACS Appl. Mater. and Interfaces* **2015**, *7*, 28420–28428.
- (45) Zhang, F.; Kahn, A. Investigation of the high electron affinity molecular dopant F6-TCNNQ for hole-transport materials. *Adv. Funct. Mater.* **2018**, *28*, 1703780.
- (46) Karpov, Y.; Erdmann, T.; Raguzin, I.; Al-Hussein, M.; Binner, M.; Lappan, U.; Stamm, M.; Gerasimov, K. L.; Beryozkina, T.; Bakulev, V. et al. High Conductivity in Molecularly p-Doped Diketopyrrolopyrrole-Based Polymer: The Impact of a High Dopant Strength and Good Structural Order. *Adv. Mater.* **2016**, *28*, 6003–6010.

- (47) Lin, X.; Purdum, G. E.; Zhang, Y.; Barlow, S.; Marder, S. R.; Loo, Y. L.; Kahn, A. Impact of a Low Concentration of Dopants on the Distribution of Gap States in a Molecular Semiconductor. *Chem. Mater.* **2016**, *28*, 2677–2684.
- (48) Pahner, P.; Kleemann, H.; Burtone, L.; Tietze, M. L.; Fischer, J.; Leo, K.; Lüssem, B. Pentacene Schottky diodes studied by impedance spectroscopy: Doping properties and trap response. *Phys. Rev. B* **2013**, *88*.
- (49) Tietze, M. L.; Burtone, L.; Riede, M.; Lüssem, B.; Leo, K. Fermi level shift and doping efficiency in p-doped small molecule organic semiconductors: A photoelectron spectroscopy and theoretical study. *Phys. Rev. B* **2012**, *86*, 035320.
- (50) Meyer, J.; Hamwi, S.; Schmale, S.; Winkler, T.; Johannes, H.-H.; Riedl, T.; Kowal-sky, W. A strategy towards p-type doping of organic materials with HOMO levels beyond 6 eV using tungsten oxide. *J. Mater. Chem* **2009**, 702–705.
- (51) Koech, P. K.; Padmaperuma, A. B.; Wang, L.; Swensen, J. S.; Polikarpov, E.; Darsell, J. T.; Rainbolt, J. E.; Gaspar, D. J. Synthesis and application of 1,3,4,5,7,8-hexafluorotetracyanonaphthoquinodimethane (F6-TNAP): A conductivity dopant for organic light-emitting devices. *Chem. Mater.* **2010**, *22*, 3926–3932.
- (52) Zhu, L.; Kim, E.-G.; Yi, Y.; Brédas, J.-L. Charge Transfer in Molecular Complexes with 2,3,5,6-Tetrafluoro-7,7,8,8-tetracyanoquinodimethane F4-TCNQ): A Density Functional Theory Study. *Chem. Mater.* **2011**, *23*, 5149–5159.
- (53) Li, J.; D’Avino, G.; Pershin, A.; Jacquemin, D.; Duchemin, I.; Beljonne, D.; Blase, X. Correlated electron-hole mechanism for molecular doping in organic semiconductors. *Phys. Rev. Mater.* **2017**, *1*, 025602.
- (54) Gaul, C.; Hutsch, S.; Schwarze, M.; Schellhammer, K. S.; Bussolotti, F.; Kera, S.; Cuniberti, G.; Leo, K.; Ortman, F. Insight into doping efficiency of organic semicon-

- ductors from the analysis of the density of states in n-doped C<sub>60</sub> and ZnPc. *Nat. Mater.* **2018**, 1.
- (55) Boltalina, O. V.; Galeva, N. A. Direct fluorination of fullerenes. *Russ. Chem. Rev.* **2007**, 69, 609–621.
- (56) Popov, A. A.; Senyavin, V. M.; Boltalina, O. V.; Seppelt, K.; Spandl, J.; Feigerle, C. S.; Compton, R. N. Infrared, Raman, and DFT vibrational spectroscopic studies of C<sub>60</sub>F<sub>36</sub> and C<sub>60</sub>F<sub>48</sub>. *J. Phys. Chem. A* **2006**, 110, 8645–52.
- (57) Boltalina, O. V.; Borschevskii, A. Y.; Sidorov, L. N.; Street, J. M.; Taylor, R. Preparation of C<sub>60</sub>F<sub>36</sub> and C<sub>70</sub>F<sub>36/38/40</sub>. *Chem. Commun.* **1996**, 529.